JACS
JOURNAL OF THE AMERICAN CHEMICAL SOCIETY

Communication

pubs.acs.org/JACS

Asymmetric Synthesis of Chiral Bimetallic $[Ag_{28}Cu_{12}(SR)_{24}]^{4-}$ Nanoclusters via Ion Pairing

Juanzhu Yan,[†,§] Haifeng Su,[†,§] Huayan Yang,[†] Chengyi Hu,[†] Sami Malola,[‡] Shuichao Lin,[†] Boon K. Teo,*[,†] Hannu Häkkinen,[‡] and Nanfeng Zheng*[,†]

[†]State Key Laboratory for Physical Chemistry of Solid Surfaces, Collaborative Innovation Center of Chemistry for Energy Materials, and Engineering Research Center for Nano-Preparation Technology of Fujian Province, College of Chemistry and Chemical Engineering, Xiamen University, Xiamen 361005, China

[‡]Departments of Physics and Chemistry, Nanoscience Center, University of Jyväskylä, FI-40014 Jyväskylä, Finland

Supporting Information

ABSTRACT: In this work, a facile ion-pairing strategy for asymmetric synthesis of optically active negatively charged chiral metal nanoparticles using chiral ammonium cations is demonstrated. A new thiolated chiral three-concentric-shell cluster, $[Ag_{28}Cu_{12}(SR)_{24}]^{4-}$, was first synthesized as a racemic mixture and characterized by single-crystal X-ray structure determination. Mass spectrometric measurements revealed relatively strong ion-pairing interactions between the anionic nanocluster and ammonium cations. Inspired by this observation, the as-prepared racemic mixture was separated into enantiomers by employing chiral quaternary ammonium salts as *chiral resolution* agents. Subsequently, direct *asymmetric synthesis* of optically active enantiomers of $[Ag_{28}Cu_{12}(SR)_{24}]^{4-}$ was achieved by using appropriate chiral ammonium cations (such as *N*-benzylcinchoninium vs *N*-benzylcinchonidinium) in the cluster synthesis. These simple strategies, ion-pairing enantioseparation and direct asymmetric synthesis using chiral counterions, may be of general use in preparing chiral metal nanoparticles.

Chirality is a fundamental property of nature ranging from the microscopic to the macroscopic world. The past two centuries have witnessed tremendous progress in understanding chirality at the molecular scale and its structure−property relationships in various technological applications.[1] Numerous chemical means have been established for the enantioselective synthesis of chiral molecules of importance in chemical,[2] agricultural,[3] materials,[4] and life science industries.[5] Many applications of nanoscaled chiral materials have been demonstrated in fundamental science and practical applications (e.g., optical devices,[6] enantioselective catalysis,[7] separation,[8] biosensing,[9] and functional self-assembly[10]). However, unlike sophisticated asymmetric syntheses of chiral molecules or assemblies of large chiral architectures (above the submicrometer scale),[11] there is currently a paucity of facile synthetic or separation methodology for chiral metal nanoclusters. With increasingly powerful experimental techniques such as X-ray diffraction and mass spectrometry,[12−23] the chirality of many nanoparticles can now be probed at the molecular level using atomically precise nanoclusters as models.

Within the class of *chiral* metal nanoclusters, four main types can be identified:[24−26] (a) the presence of chiral ligands through vicinal effects or through a chiral electrostatic field; (b) asymmetric arrangement of achiral ligands to form a chiral shell; (c) inherently chiral metal framework; and (d) distortion of the structure, which lowers the symmetry of the cluster to a chiral point group. The majority of chiral metal nanoclusters known to date are of types (a)[27−36] and (b),[16,17,37−39] with a few belonging to types (c) and (d).[40−42] As prepared, many of these chiral metal nanoclusters (types b−d) are racemic mixtures that require separation and purification by various optical resolution methods. Enantioseparation of Au nanoclusters (e.g., Au_{28}, Au_{38}, Au_{40}) has been reported by using chiral HPLC columns.[43−45] For example, Knoppe et al. separated Au_{102} enantiomers by a phase transfer method using a chiral ammonium salt.[46] In this communication, we wish to demonstrate a facile technique for achieving chirality by enantioseparation of a racemic mixture of a new chiral metal nanocluster via ion pairing with a chiral counterion. Subsequent asymmetric synthesis of optically active enantiomers was first achieved by employing chiral counterions in the synthesis.

Specifically, we report herein the synthesis of a new chiral thiolated bimetallic cluster, $[Ag_{28}Cu_{12}(SR)_{24}]^{4-}$ (**1**), where SR = 2,4-dichlorobenzenethiol, its chiral separation and asymmetric synthesis via ion-pairing with chiral quaternary ammonium salts. The 28 Ag atoms in the cluster are arranged in a distorted face-centered cubic (*fcc*) pattern, while the Ag/Cu interface in distorted hexagonal close packing (*hcp*). The distortions lower the point-group symmetry of the $Ag_{28}Cu_{12}$ framework from T_d to T, turning it into a chiral cluster. When nonchiral counter cations were used, the as-prepared chiral cluster was a racemic mixture. By capitalizing on the strong ion pairing between the chiral cluster and the counterions, the racemic mixture can readily be separated into enantiomers by employing chiral quaternary ammonium salts, such as *N*-benzylcinchonidinium chloride (BCDC), and *N*-benzylcinchoninium chloride (BCNC), as *resolution* agents. Subsequent *asymmetric synthesis* of the chiral cluster **1** using chiral ammonium salts, BCDC and BCNC, gave rise to optically active enantiomers separately.

Received: August 4, 2016
Published: September 14, 2016

DOI: 10.1021/jacs.6b08100
J. Am. Chem. Soc. 2016, 138, 12751−12754

To prepare thiolated Ag−Cu bimetallic nanoparticles, the metal precursors (i.e., $AgNO_3$, CuBr) were chemically reduced by $NaBH_4$ in the presence of 2,4-dichlorobenzenethiol (HSR), tetrabutylammonium bromide ($^nBu_4NBr$ or TBAB), and triethylamine in a mixed solvent of methanol and dichloromethane at 0 °C (see SI for details). Transmission electron microscopic (TEM) analyses revealed that the as-prepared AgCu nanoparticles had a uniform size of 2.06 ± 0.22 nm (Figure S1). Single-crystal X-ray structure determination revealed that the

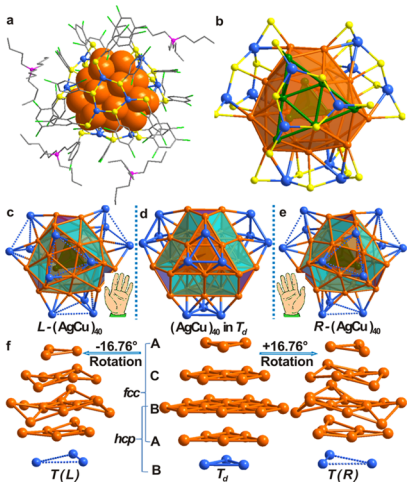

Figure 1. (a) Overall structure of $(^nBu_4N)_4[Ag_{28}Cu_{12}(SR)_{24}]$ (**1**·TBA). (b) Cluster **1** with the R groups omitted for clarity. (c,e) A pair of enantiomers of **1** having the chiral $Ag_{28}Cu_{12}$ metal frameworks with *T* symmetry. (d) Idealized *fcc* close-packing of the corresponding (hypothetical) achiral $Ag_{28}Cu_{12}$ metal framework with T_d symmetry. (f) ACBAB stacking of Ag and Cu atoms: middle, idealized T_d symmetry (ACBA of the Ag_{28} is *fcc* and BAB of the Ag−Cu interface is *hcp*); left and right, observed layer stacking in *T* symmetry of left- and right-handed isomers of **1**, respectively. Color codes: orange, Ag; blue, Cu; yellow, S; green, Cl; Pink, N; gray, C. Hydrogen atoms are omitted for clarity.

formulation of $[Ag_{28}Cu_{12}(SR)_{24}]^{4-}$ (**1**) (Figure 1a), as the $^nBu_4N^+$ salt, which crystallizes in a monoclinic cell of $P2_1/n$ space group. The unit cell comprises two pairs ($Z = 4$) of enantiomeric nanoclusters **1** and 16 cations (Figure S2).

A detailed analysis of the structure of $[Ag_{28}Cu_{12}(SR)_{24}]^{4-}$ (**1**) revealed a two-shell $Ag_4@Ag_{24}$ core protected by four nearly planar $Cu_3(SR)_6$ moieties. The $Ag_4@Ag_{24}$ core can be described as an inner ν_1 tetrahedral Ag_4 core capped on its four faces by four ν_2 triangular Ag_6 facets in a slightly angular twist (Figure S3a).[47] The four Ag_6 facets are interconnected to form the Ag_{24} shell, which is capped by four $Cu_3(SR)_6$ moieties in a tetrahedral fashion to form the outer surface layer (Figure 1b). The Cu atoms are three-coordinated by thiolates. The pairwise $\pi\cdots\pi$ interactions between the six thiolates of $Cu_3(SR)_6$ motifs are clearly revealed on the surface of **1** (Figure S3b). The Cu and S atoms in the $Cu_3(SR)_6$ moieties are practically coplanar. As a result, all the Cu atoms in the title cluster are partially exposed, which might be of use as *in situ* active sites or reactive centers in catalysis.

Further analysis of the $Ag_4@Ag_{24}$ kernal revealed that it resembles a ν_5 tetrahedron truncated at four vertices (first truncation) and six edges (second truncation).[47] The four ν_2 triangular Ag_6 facets thus formed are further capped by four $Cu_3(SR)_6$ units, as portrayed in Figure 1d. The resulting geometry conforms to the T_d symmetry. Concerted rotations of the two outer shells, viz., four $Ag_6@Cu_3$ moieties by 16.76° (with respect to the inner ν_1 tetrahedral Ag_4 core) about the 3-fold axes lower the symmetry to the chiral *T* point group of the observed structure. Due to these rotations, each of the rectangular faces in Figure 1d turns into two triangles in Figure 1c,e, resulting in a wide range of the Ag−Ag distances from 2.698 to 3.128 Å between Ag_4 tetrahedron and the Ag_{24} shell. As shown in Figure 1f (middle), the ACBA *fcc* stacking of the layers in the idealized Ag_{28} kernal of T_d symmetry is capped at the bottom by a Cu_3 overlayer, making the Ag−Cu interface a BAB hexagonal close-packing (*hcp*) arrangement. Thus, the $Ag_{24}Cu_{12}$ framework of idealized T_d symmetry exhibits a mixed *fcc*/hcp stacking sequence of ACBAB. The corresponding distorted layer stacking of cluster **1** is depicted in Figure 1f (left and right). It conforms to chiral *T* symmetry.

The UV−vis spectra (Figure 2a) of both the as-prepared nanoparticles and their single crystals dissolved in CH_2Cl_2

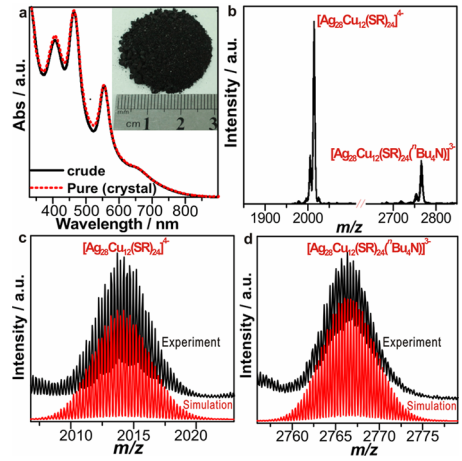

Figure 2. (a) Comparison of UV−vis spectra of single crystals of $(^nBu_4N)_4[Ag_{28}Cu_{12}(SR)_{24}]$ (**1**·TBA) and the as-prepared crude product dissolved in CH_2Cl_2. Inset shows photo of 1.2 g of **1**·TBA in a scale-up reaction. (b) ESI−MS of single-crystals of **1**·TBA in CH_2Cl_2. (c,d) Comparison of the experimental (in black) and simulated (in red) isotopic patterns of the MS of $[Ag_{28}Cu_{12}(SR)_{24}]^{4-}$ (c) and $[Ag_{28}Cu_{12}(SR)_{24}(^nBu_4N)]^{3-}$ (d).

displayed four bands at 407, 465, 555, and 653 nm (shoulder). The Lambert−Beer plot of **1**·TBA is shown in Figure S4. Both products were also characterized by electrospray ionization mass spectrometry (ESI−MS) (Figure 2b). As depicted in Figure 2c,d, the high-resolution mass spectra of **1**·TBA revealed a perfect match between the observed and the simulated isotopic distribution of $[Ag_{28}Cu_{12}(SR)_{24}]^{4-}$ and $[Ag_{28}Cu_{12}(SR)_{24}(TBA)]^{3-}$ peaks. Both UV−vis and ESI−MS results clearly indicated the presence of high-purity $[Ag_{28}Cu_{12}(SR)_{24}]^{4-}$ in the crude product, making it easy to synthesize the nanoclusters in gram-scale (inset, Figure 2a). The high-yield synthesis of $[Ag_{28}Cu_{12}(SR)_{24}]^{4-}$ is due to its good stability of **1**, which can be attributed to its 20 electron count (i.e., 28 + 12 − 24 + 4 = 20) being in accordance with the Jelliumatic closed-shell electronic configuration of $1S^21P^61D^{10}2S^2$ (Figure S5, see SI for computational details).

As prepared **1** using achiral countercation, TBA^+, is a racemic mixture, both in solution and in crystal form. In view of the relatively strong ion pairing between the anionic cluster and the countercation, TBA^+, revealed by ESI−MS (Figure 2d), it

DOI: 10.1021/jacs.6b08100
J. Am. Chem. Soc. 2016, 138, 12751−12754

occurred to us that it may be possible to use chiral quaternary ammonium cations to separate the two enantiomers. Since chiral quaternary ammonium halides such as BCNC and BCDC (Figure S6) are widely used in various asymmetric reactions as phase transfer catalysts, they were selected for the enantioseparation. Experimentally, in order to exclude the influence of strong ion paring between **1** and TBA^+, the racemates of **1**·Na(H) were first prepared as described above by excluding TBA. The as-prepared **1** solution was then treated with a solution of BCNC in CH_2Cl_2. The resulting mixture was monitored by UV−vis, CD, and ESI−MS spectra as a function of time.

As shown in Figure 3a,b, the intensity of CD signal of the mixture was found to increase gradually, while its UV−vis

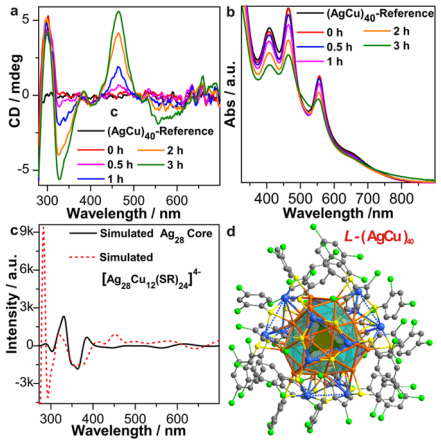

Figure 3. (a,b) Time tracking of CD spectra (a) and UV−vis (b) spectra during chiral separation in air at 0 °C; (c) calculated CD spectra of the cluster **1** (red curve) and the bare Ag_{28} core (black curve), both conforming to *T* symmetry. (d) The DFT optimized L-enantiomer of **1** used in panel c (L-$(AgCu)_{40}$ defined as the left-handed distortion of $Ag_{24}@Cu_{12}$ shells with respect to the ν_1 tetrahedral Ag_4 core, see SI for computational details). Color codes: orange, Ag; blue, Cu; yellow sphere, S; green, Cl; Pink, O, red; N; gray, C. Hydrogen atoms are omitted for clarity.

absorption diminished concomitantly. The mixture exhibited increasing CD signals (from zero), with two strong bands at 330 and 465 nm, weak peaks at 385, and 406 nm, and two broad peaks at 585 and 687 nm. Note that both BCNC and BCDC in CH_2Cl_2 exhibit only CD optical activity below 322 nm (Figure S7). The corresponding ESI−MS (Figure S8) showed the peaks of ion pairs consisting of **1** and BCNC, which suggested the increasing CD signals originated from **1**·BCNC. A comparison of the experimental and theoretical circular dichroism (CD) spectra (Figure 3a,c) showed good agreement, allowing the identification of the cluster as L-$(AgCu)_{40}$ (Figure 3d). A detailed analysis of the CD signals revealed that the chirality of **1** stems from the asymmetric stereochemistry of the bare Ag_{28} core. Interestingly, there is a linear correlation between the enhancement of the CD signal and the weakening of the UV−vis absorption (Figure S9a). In other words, one of the enantiomers in the racemate disappears more easily, while the other remains relatively stable due to steric mis-matching and matching, respectively, as a result of ion pairing between the cluster and the chiral cation. The enantiomer with steric mismatching was destroyed by air oxidation as well as by reaction with halides present in the solution during the enantioseparation process. Based on the increased CD and the decreased UV−vis absorption, the anisotropy factor of the chiral cluster was estimated to be $\sim 1 \times 10^{-3}$ at 465 nm (Figure S9b). Though quite stable in solid-state in months (Figure S10) and reasonably stable in solution in hours (Figure S11) at room temperature, $[Ag_{28}Cu_{12}(SR)_{24}]^{4-}$ in solutions was degraded in a rather fast rate by air in the presence of halides even at 0 °C (Figure S12). Indeed, the time-dependent ESI−MS (Figure S8) showed gradually diminishing signals of the parent peaks $[Ag_{28}Cu_{12}(SR)_{24}]^{4-}$ (**1**) and $[Ag_{28}Cu_{12}(SR)_{24}H]^{3-}$ when BCNC was introduced. These latter observations strongly suggested that one enantiomer of the racemic mixture was being stabilized by the chiral counter cation as a result of steric matching. On the basis of these results, the resolution of L-$(AgCu)_{40}$ from the racemic mixture can be attributed to the selective stabilizing effect of BCNC on L-$(AgCu)_{40}$ due to their stereochemically matched ion pairing. Similarly, the use of BCDC allows the separation of R-$(AgCu)_{40}$ from the racemic mixture.

Though nearly optically active enantiomer of **1** can be obtained by the above enantioseparation technique, the maximum theoretical yield is 50% (one-half of the racemic mixture). In order to overcome this disadvantage, we attempted the asymmetric synthesis of enantiomers by substituting BCDC or BCNC in place of ^{n}Bu_4NBr in the synthesis. Indeed, this turned out to be successful. The resulting respective enantiomers, **1**·BCDC and **1**·BCNC, were characterized by UV−vis (Figure S13), CD and ESI−MS (Figure 4) spectros-

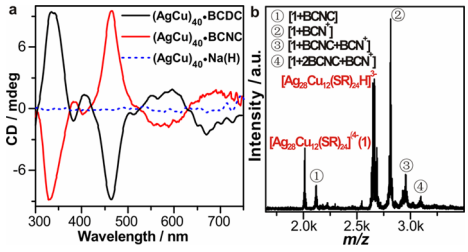

Figure 4. (a) CD spectra of CH_2Cl_2 solutions of the enantiomeric pair **1**·BCDC and **1**·BCNC as well as of **1**·Na(H), synthesized by substituting BCDC and BCNC in place of ^{n}Bu_4NBr as the counter cation, respectively (**1** is abbreviated here as $(AgCu)_{40}$). (b) ESI−MS spectrum of crude product of **1**·BCNC (*N*-benzylcinchoninium cation abbreviated as BCN^+).

copies. The UV−vis spectra are in agreement with that of **1**. CD spectra of **1**·BCDC and **1**·BCNC exhibited mirror-image CD signals in the visible range. In contrast, the CD of $[Na(H)]_4[Ag_{28}Cu_{12}(SR)_{24}]$ in CH_2Cl_2 instead showed no signals, confirming that it was indeed a racemic mixture. However, more work is still required to quantitatively determine the selectivity of the asymmetric synthesis induced by the ion pairing.

In conclusion, a new mixed-metal nanocluster, $[Ag_{28}Cu_{12}(SR)_{24}]^{4-}$ (**1**) as the ^{n}Bu_4N^+ salt, was synthesized and characterized by single-crystal X-ray structure determination, ESI−MS, and UV−vis spectroscopies. The tetraanionic cluster can be described as a chiral three concentric core−shell structure of $Ag_4@Ag_{24}@Cu_{12}(SR)_{24}$. The Ag atoms are arranged in approximately face-centered cubic (*fcc*) pattern and the Ag−Cu interface in distorted hexagonal close-packing (*hcp*). The exposed Cu atoms of the four $Cu_3(SR)_6$ units on the surface, along with *T* point-group symmetry and the associated chirality, raises the prospects of the utility of the title cluster in chiral reactions or chiral catalysis. Considering the unique interaction between the cluster and the counterion ^{n}Bu_4N^+, chiral quaternary

DOI: 10.1021/jacs.6b08100
J. Am. Chem. Soc. 2016, 138, 12751−12754

ammonium halides were introduced as chiral resolving agents, which successfully enantioseparated the racemate of **1**. Subsequent asymmetric synthesis of optically active enantiomers of **1** was achieved by using chiral phase transfer catalysts BCDC or BCNC as the counter cations. It is hoped that these two simple techniques, postsynthesis *enantioseparation* and direct *asymmetric synthesis*, for preparing optically pure chiral nanoclusters via ion pairing with a chiral counterion will find applications in the separation or synthesis of other chiral metal clusters of importance in fields such as catalysis and drug manufacturing.

■ ASSOCIATED CONTENT

Supporting Information

The Supporting Information is available free of charge on the ACS Publications website at DOI: 10.1021/jacs.6b08100.

Experimental details, computational details, analysis of the cluster electronic structure, and more mass spectra (PDF)
Detailed crystallographic structure and data (CIF)

■ AUTHOR INFORMATION

Corresponding Authors

*nfzheng@xmu.edu.cn
*boonkteo@xmu.edu.cn

Author Contributions

§J.Z.Y. and H.F.S. contributed equally to this work.

Notes

The authors declare no competing financial interest.

■ ACKNOWLEDGMENTS

We thank the MOST of China (2015CB932303) and the NNSF of China (21420102001, 21131005, 21390390, 21227001, 21333008) for financial support. The financial support (to B.K.T.) from iChEM, Xiamen University is gratefully acknowledged. We also thank Prof. H. Zhang for helpful discussions. The work in University of Jyväskylä was supported by the Academy of Finland (projects 266492, 294217 and Academy Professorship to H.H.). The computations were made at the CSC computing center in Espoo, Finland.

■ REFERENCES

(1) Lough, W. J.; Wainer, I. W. *Chirality in Natural and Applied Science*; CRC Press/Wiley-Blackwell Pub.: Osney Mead, Oxford, 2002.
(2) Soai, K.; Shibata, T.; Morioka, H.; Choji, K. *Nature* **1995**, *378*, 767.
(3) Lewis, D. L.; Garrison, A. W.; Wommack, K. E.; Whittemore, A.; Steudler, P.; Melillo, J. *Nature* **1999**, *401*, 898.
(4) Oda, R.; Huc, I.; Schmutz, M.; Candau, S. J.; MacKintosh, F. C. *Nature* **1999**, *399*, 566.
(5) Schmid, A.; Dordick, J. S.; Hauer, B.; Kiener, A.; Wubbolts, M.; Witholt, B. *Nature* **2001**, *409*, 258.
(6) Zhao, Y.; Belkin, M. A.; Alù, A. *Nat. Commun.* **2012**, *3*, 870.
(7) Mallat, T.; Orglmeister, E.; Baiker, A. *Chem. Rev.* **2007**, *107*, 4863.
(8) Hare, P. E.; Gil-Av, E. *Science* **1979**, *204*, 1226.
(9) Torsi, L.; Farinola, G. M.; Marinelli, F.; Tanese, M. C.; Omar, O. H.; Valli, L.; Babudri, F.; Palmisano, F.; Zambonin, P. G.; Naso, F. *Nat. Mater.* **2008**, *7*, 412.
(10) Kuzyk, A.; Fan, Z.; Pardatscher, G.; Roller, E.; Hogele, A.; Simmel, F. C.; Govorov, A. O.; Liedl, T. *Nature* **2012**, *483*, 311.
(11) Cornelissen, J. J. L. M.; Rowan, A. E.; Nolte, R. J. M.; Sommerdijk, N. A. J. M. *Chem. Rev.* **2001**, *101*, 4039.
(12) Jin, R. C. *Nanoscale* **2015**, *7*, 1549.
(13) Teo, B. K.; Zhang, H. *Proc. Natl. Acad. Sci. U. S. A.* **1991**, *88*, 5067.
(14) Negishi, Y.; Takasugi, Y.; Sato, S.; Yao, H.; Kimura, K.; Tsukuda, T. *J. Am. Chem. Soc.* **2004**, *126*, 6518.
(15) Luo, Z.; Nachammai, V.; Zhang, B.; Yan, N.; Leong, D. T.; Jiang, D.; Xie, J. *J. Am. Chem. Soc.* **2014**, *136*, 10577.
(16) Jadzinsky, P. D.; Calero, G.; Ackerson, C. J.; Bushnell, D. A.; Kornberg, R. D. *Science* **2007**, *318*, 430.
(17) Qian, H. F.; Eckenhoff, W. T.; Zhu, Y.; Pintauer, T.; Jin, R. C. *J. Am. Chem. Soc.* **2010**, *132*, 8280.
(18) Yang, H. Y.; Wang, Y.; Huang, H. Q.; Gell, L.; Lehtovaara, L.; Malola, S.; Häkkinen, H.; Zheng, N. F. *Nat. Commun.* **2013**, *4*, 2422.
(19) Desireddy, A.; Conn, B. E.; Guo, J.; Yoon, B.; Barnett, R. N.; Monahan, B. M.; Kirschbaum, K.; Griffith, W. P.; Whetten, R. L.; Landman, U.; Bigioni, T. P. *Nature* **2013**, *501*, 399.
(20) Wang, Y.; Su, H. F.; Xu, C. F.; Li, G.; Gell, L.; Lin, S. C.; Tang, Z. C.; Häkkinen, H.; Zheng, N. F. *J. Am. Chem. Soc.* **2015**, *137*, 4324.
(21) Wang, Y.; Wan, X. K.; Ren, L. T.; Su, H. F.; Li, G.; Malola, S.; Lin, S. C.; Tang, Z. C.; Häkkinen, H.; Teo, B. K.; Wang, Q. M.; Zheng, N. F. *J. Am. Chem. Soc.* **2016**, *138*, 3278.
(22) Yang, H. Y.; Wang, Y.; Yan, J. Z.; Chen, X.; Zhang, X.; Häkkinen, H.; Zheng, N. F. *J. Am. Chem. Soc.* **2014**, *136*, 7197.
(23) Zhang, X.; Yang, H. Y.; Zhao, X. J.; Wang, Y.; Zheng, N. F. *Chin. Chem. Lett.* **2014**, *25*, 839.
(24) Gautier, C.; Burgi, T. *ChemPhysChem* **2009**, *10*, 483.
(25) Noguez, C.; Garzon, I. L. *Chem. Soc. Rev.* **2009**, *38*, 757.
(26) Knoppe, S.; Burgi, T. *Chimia* **2013**, *67*, 236.
(27) Schaaff, T. G.; Knight, G.; Shafigullin, M. N.; Borkman, R. F.; Whetten, R. L. *J. Phys. Chem. B* **1998**, *102*, 10643.
(28) Schaaff, T. G.; Whetten, R. L. *J. Phys. Chem. B* **2000**, *104*, 2630.
(29) Yao, H.; Miki, K.; Nishida, N.; Sasaki, A.; Kimura, K. *J. Am. Chem. Soc.* **2005**, *127*, 15536.
(30) Gautier, C.; Burgi, T. *Chem. Commun.* **2005**, 5393.
(31) Gautier, C.; Taras, R.; Gladiali, S.; Burgi, T. *Chirality* **2008**, *20*, 486.
(32) Knoppe, S.; Dharmaratne, A. C.; Schreiner, E.; Dass, A.; Burgi, T. *J. Am. Chem. Soc.* **2010**, *132*, 16783.
(33) Zhu, M. Z.; Qian, H. F.; Meng, X. M.; Jin, S. S.; Wu, Z. K.; Jin, R. C. *Nano Lett.* **2011**, *11*, 3963.
(34) Knoppe, S.; Kothalawala, N.; Jupally, V. R.; Dass, A.; Burgi, T. *Chem. Commun.* **2012**, *48*, 4630.
(35) Yanagimoto, Y.; Negishi, Y.; Fujihara, H.; Tsukuda, T. *J. Phys. Chem. B* **2006**, *110*, 11611.
(36) Provorse, M. R.; Aikens, C. M. *J. Am. Chem. Soc.* **2010**, *132*, 1302.
(37) Zeng, C. J.; Chen, Y. X.; Kirschbaum, K.; Appavoo, K.; Sfeir, M. Y.; Jin, R. C. *Sci. Adv.* **2015**, *1*, e1500045.
(38) Dass, A.; Theivendran, S.; Nimmala, P. R.; Kumara, C.; Jupally, V. R.; Fortunelli, A.; Sementa, L.; Barcaro, G.; Zuo, X.; Noll, B. C. *J. Am. Chem. Soc.* **2015**, *137*, 4610.
(39) Yan, J. Z.; Su, H. F.; Yang, H. Y.; Malola, S.; Lin, S. C.; Häkkinen, H.; Zheng, N. F. *J. Am. Chem. Soc.* **2015**, *137*, 11880.
(40) Zeng, C. J.; Chen, Y. X.; Liu, C.; Nobusada, K.; Rosi, N. L.; Jin, R. C. *Sci. Adv.* **2015**, *1*, e1500425.
(41) Hakkinen, H.; Moseler, M.; Kostko, O.; Morgner, N.; Hoffmann, M. A.; Issendorff, B. v. *Phys. Rev. Lett.* **2004**, *93*, 093401.
(42) Garzon, I. L.; Beltran, M. R.; Gonzalez, G.; Gutierrez-Gonzalez, I.; Michaelian, K.; Reyes-Nava, J. A.; Rodriguez-Hernandez, J. I. *Eur. Phys. J. D* **2003**, *24*, 105.
(43) Dolamic, I.; Knoppe, S.; Dass, A.; Burgi, T. *Nat. Commun.* **2012**, *3*, 798.
(44) Zeng, C.; Li, T.; Das, A.; Rosi, N. L.; Jin, R. C. *J. Am. Chem. Soc.* **2013**, *135*, 10011.
(45) Knoppe, S.; Dolamic, I.; Dass, A.; Bürgi, T. *Angew. Chem., Int. Ed.* **2012**, *51*, 7589.
(46) Knoppe, S.; Wong, O. A.; Malola, S.; Häkkinen, H.; Bürgi, T.; Verbiest, T.; Ackerson, C. J. *J. Am. Chem. Soc.* **2014**, *136*, 4129.
(47) Teo, B. K.; Sloane, N. J. A. *Inorg. Chem.* **1985**, *24*, 4545.

DOI: 10.1021/jacs.6b08100
J. Am. Chem. Soc. 2016, 138, 12751−12754